Efficient spin transfer torque in $La_{2/3}Sr_{1/3}MnO_3$ nanostructures

Michael Foerster,[1,2] Luis Peña,[1] C. A. F. Vaz,[1,3] Jan Heinen,[4] Simone Finizio,[1] Tomek Schulz,[1] André Bisig,[1] Felix Büttner,[1,5] Stefan Eisebitt,[5] Laurence Méchin,[6] Sebastian Hühn,[7] Vasily Moshnyaga,[7] and Mathias Kläui[1,3,4]

[1]*Institut für Physik, Johannes Gutenberg-Universität, Staudingerweg 7, 55128 Mainz, Germany*
[2]*ALBA Synchrotron light source, Carrretera BP 1413, km 3.3, 08290 Cerdanyola del Valles, Barcelona, Spain*
[3]*SwissFEL, Paul Scherrer Institut, 5232 Villigen PSI, Switzerland*
[4]*Fachbereich Physik, Universität Konstanz, Universitätsstraße 10, 78457 Konstanz, Germany*
[5]*Institut für Optik und Atomare Physik, Technische Universität Berlin, Straße des 17. Juni 135, 10623 Berlin, Germany*
[6]*GREYC, UMR 6072, CNRS-ENSICAEN-UCBN, 6 Boulevard du Maréchal Juin, Caen Cedex 14050, France*
[7]*Georg-August-Universität Göttingen, Friedrich-Hund-Platz 1, 37077 Göttingen, Germany*

(Received 20 September 2013; accepted 7 January 2014; published online 19 February 2014)

We carry out low temperature magnetotransport measurements on nanostructured $La_{2/3}Sr_{1/3}MnO_3$ wires to study the interaction between spin-polarized current and magnetization in this half metallic material. We selectively position domain walls by applying external fields. The domain wall resistance is found to be positive, in contrast to conventional 3*d* metals. The depinning field is reduced when current pulses are injected into the wire. By comparing measurements for both current polarities, we can disentangle heating and spin transfer torque effects. The determined spin transfer torque efficiency is of the order of 4×10^{-14} Tm^2/A, which is significantly higher than in permalloy. © *2014 AIP Publishing LLC*. [http://dx.doi.org/10.1063/1.4865415]

The conventional switching of magnetic devices by external magnetic fields is well established but known to exhibit poor scaling behavior. Thus, for next generation magnetic devices, the interaction between spin polarized current and magnetization through the spin transfer torque (STT) is expected to be used for low power magnetization manipulation. The possibility to manipulate magnetization in confined geometries by the injection of spin polarized currents due to the transfer of spin angular momentum from electrons to the magnetization has been predicted theoretically some time ago.[1,2] This approach exhibits favorable scaling, as the relevant current density for switching is constant, leading to reduced power consumption for a decreasing device design rule. Experimentally, this effect was confirmed for nanopillar structure switching[3] and for current-induced domain wall motion.[4–6] This approach was quickly transferred to industrial devices and the effect is now used in nanopillar-based memory applications (STT magnetic random access memory, STT-MRAM for instance by Everspin Technologies).

Also memory devices based on current-induced domain wall motion have been proposed, such as the racetrack memory and related concepts[7,8] where bits of information are represented by magnetic domains in a nanowire. To address a relevant bit, the domains and domain walls are shifted synchronously along a magnetic nanowire by an injected spin-polarized current to the read or write unit.

So far, much research on STT effects has focused on 3*d* metals (for an overview see for instance[9]), as the domain and spin structures in these materials are well established. However, the high critical current densities necessary for wall motion have been a major stumbling block for the development of industrially relevant devices.

In general the spin torque efficiency is strongly material dependent, opening possibilities by exploring other, advanced materials. Materials with high spin polarization P such as half metals and materials with a low saturation magnetization M_S promise a high spin transfer torque efficiency and thus efficient magnetization manipulation as the spin transfer torque efficiency scales with P/M_s.[10]

STT in a few highly spin-polarized materials have been investigated including CrO_2.[11] However, one key problem has been that many half metallic materials exhibit large magnetocrystalline anisotropies leading to difficulties in controlling the spin structure of domains and domain walls.[11,12] $La_{2/3}Sr_{1/3}MnO_3$ (LSMO) is a promising half-metallic material that in recent experiments with geometrically confined structures has shown a low magnetocrystalline anisotropy, allowing one to tailor the spin structure and displace domain walls with low pinning.[13,14] Furthermore, the moderately high Curie temperature ($T_C \approx 360$ K for thin films),[15] which is above room temperature, allows one to study STT even close to the magnetic phase transition where material parameters like the saturation magnetization M_S reach effectively zero, adding an additional experimentally tunable parameter. So far, reports on the interaction of spin-polarized charge carriers and magnetization (including STT) in LSMO or related perovskites are indirect[16,17] or at relatively high current densities in point contacts[18] and, given the promising prerequisites, a motivation for studying this material has become clear.

In this Letter, we use low temperature magnetoresistance measurements to investigate LSMO nanostructures in which magnetic domain walls are controllably positioned. We identify the resistance contribution associated to a magnetic domain wall and use it to measure the critical field necessary for moving a domain wall as function of injected current pulse magnitude. Comparing the results for both current directions, we are able to discriminate STT effects from current induced (Joule) heating and quantify the STT efficiency. We find a high efficiency compared to conventional

magnetic materials in line with the half-metallic properties in LSMO. Due to the relatively high resistivity, strong Joule heating in combination with the relatively moderate T_C leads to changes in the magnetization configuration for higher current densities.

LSMO thin films with thickness $t = 30$ nm for this study were grown by pulsed laser deposition (PLD)[19] and metalorganic aerosol deposition (MAD)[20] onto single crystalline $SrTiO_3$ (001) substrates. Detailed deposition conditions and characterization can be found elsewhere.[19,20] LSMO half ring structures (width $w = 0.5$–$2\,\mu$m, length l around $20\,\mu$m) and electrodes for transport measurements were patterned by electron beam lithography and subsequent Ar ion milling. The half ring geometry was chosen as it allows one to selectively position domain walls at different positions by applying fields along different directions.[21] Magnetotransport measurements were performed in a variable temperature insert He cryostat with a 3D vector-magnet. Measurements at 4.2 K were taken with the sample volume flooded with liquid He to assure temperature stability. The resistive signal of the wire was measured in a four contact scheme (see inset in Figure 1 for a schematic depiction) by an AC modulation technique using lock-in detection of the voltage signal at the two inner contacts (V+ and V−), while the current was injected into the outer two contacts (I+ and I−). To improve the sensitivity to small resistance changes, the signal was partially compensated by subtracting the signal from a serial ohmic resistance using two SRS 560 preamplifiers. The LSMO wire resistivity is around $900\,\mu\Omega$ cm at 300 K, decreasing to around $100\,\mu\Omega$ cm at 4.2 K. Current pulses were injected using an Agilent 33250a pulse generator producing rectangular voltage pulses between −9 V and +9 V, which translates to current densities of up to +/− 36 GA/m^2 based on the resistivity at 4.2 K. The pulse duration was $10\,\mu$s with hundreds of μs waiting time between the pulses to ensure the return to the equilibrium temperature between pulses.

The anisotropic magnetoresistance (AMR) was measured in saturating fields (0.3 T and 1 T) at 4.2 K, sweeping the angle between current (i.e., the half ring wire) and field; the ratio {R(H || I)-R(H ∟ I)}/R(H || I) is −1.3%.[22] That AMR value, in line with previous reports,[23] exhibits the opposite sign to that in 3*d* metals (Py, Co, etc.) and this sign change is also found for instance in Ir doped permalloy.[24]

We first determine the position of the domain wall by transport measurements. For that we rely on the established "star mode" measurement scheme:[21] In Figure 1, we show the remanent (H = 0) resistance of the LSMO wire after applying and relaxing a saturating field as function of the direction of that field, measured at 4.2 K. With this method, we position the domain wall at the angle corresponding to the direction of the applied field which is then at zero before the resistance measurement. The resistance values in Fig. 1 have been obtained by averaging data from measurements with increasing and decreasing angle. It is observed that for angles between 10° and 25° the resistance after relaxing the field back to zero is clearly higher than for other angles. This increase of around 0.5 Ω (or 0.16%) is a signature of the presence of a magnetic domain wall nucleated in the area between the contacts. We have imaged similar LSMO wire structures using photo emission electron microscopy with X-ray circular dichroism (XMCD-PEEM) to achieve magnetic contrast,[22] showing the presence of magnetic domain walls after an equivalent field ramping. Since such a domain wall contains regions with magnetization perpendicular to the wire, the AMR effect described above is expected to result in an increase in the wire resistance as indeed experimentally observed. So we conclude from this data that a magnetic domain wall structure can be reproducibly nucleated in the LSMO wire and detected by a resistance measurement.

The magnetic domain walls can then be displaced by the application of a magnetic field along a direction tangential to the half ring at the domain wall position. This field moves the wall outside the half ring leading to a quasi-single domain state.[25] We detect this domain wall motion process by monitoring the wire resistance while slowly ramping up the magnetic field in small steps. Figure 2 shows that the domain wall is driven out of the measured region between the two inner voltage contacts at a field between 10 and 15 mT with

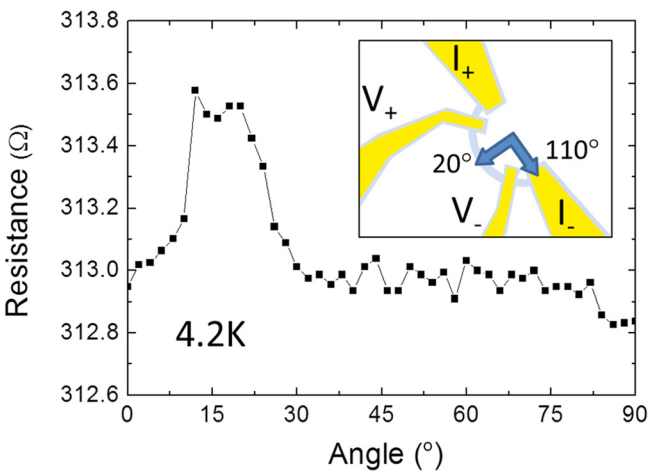

FIG. 1. Measurement of the resistance of the LSMO half ring as a function of the angular domain wall position. For directions between 10° and 25° (see inset), an increase of the resistance is observed, corresponding to a magnetic domain wall positioned between the two inner contacts of the wire.

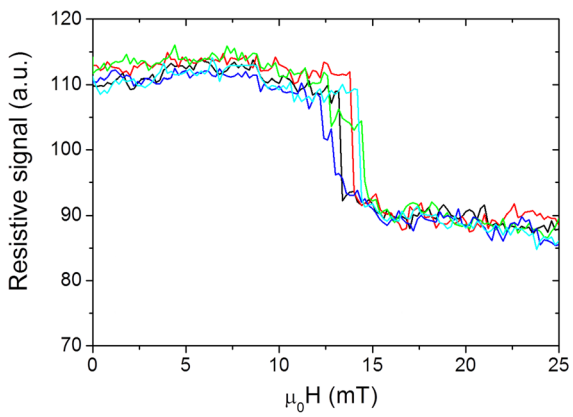

FIG. 2. Resistance signal of the probed part of the half ring LSMO structure (inset of Figure 1), as function of an increasing tangential magnetic field. Prior to each measurement, a magnetic domain wall was nucleated by a perpendicular magnetic field. The drop of the signal around 13 mT corresponds to the depinning and removal of the magnetic domain wall from the wire. The different colours correspond to multiple measurements revealing a typical depinning field distribution.

some stochasticity due to thermal activation leading to a switching field distribution. This depinning field is necessary to overcome the pinning of the domain walls at natural pinning sites that can arise, e.g., from unavoidable edge irregularities or local variations in materials properties for instance due to defects in the crystalline structure. Thus, once a sufficient magnetic field is applied to overcome the strength of the strongest pinning sites within the probed segment of the half ring, the measured resistance drops instantaneously as the domain wall is driven out of the probed area. This behavior was then analyzed to determine the switching fields. For the analysis, we measure the detected depinning events, as shown in Figure 2 as a function of injected current.

These experiments were repeated for different angles, all showing similar results when the angle of the saturation field is between 13° and 24° (directions for which the domain wall is nucleated in the probed area between the voltage contacts, see Fig. 1) with the corresponding depinning field perpendicular to the saturation field.

Having established the controlled nucleation and depinning of a domain wall, we use the current-field equivalence[26,27] of the depinning process to determine the spin torque efficiency in this material. The injection of the spin-polarized electrons exerts a torque on a domain wall, reducing the depinning field. The non-adiabatic part of this torque acts as an effective field which in combination with an external field is used to move the domain wall out of the probed part of the LSMO half ring. For each measurement, we first reset the magnetic structure in the half ring by applying a field of at 0.3 T along the half ring (110°, see Fig. 1). Then we nucleate a magnetic domain wall as described before (field direction 20°). Then we start at zero field and again ramp up the tangential magnetic field (in small field steps of 0.2 mT along 110°), while applying at each step, at constant field, three current pulses with a given current density before measuring the resistance to determine whether the domain wall has been moved. From the jump of the resistance signal, which typically occurred within one field step, the depinning field was determined.

In Figure 3, we show the averaged data for the current assisted depinning field for different experimental runs, where error bars represent one standard deviation. Two different regimes are identified: First, at small current densities (voltage pulses of 0 to −/+ 2 V, corresponding to approx. 0–8 GA/m^2), the depinning field decreases for both current polarities in a very similar way as also previously observed in 3*d* metals.[28] Clearly, this symmetric reduction for both current polarities cannot be ascribed to spin torque effects, but most likely results from a polarity-independent heating of the LSMO wire by the current pulse. Second, at higher current densities above approximately 8 GA/m^2, a further reduction is observed for positive currents only. To validate this, we have performed a number of fits of this high current density data for symmetric (identical for positive and negative current densities, dotted line in Fig. 3) and asymmetric (constant depinning field for negative (dashed line) and a linearly varying depinning field for positive current densities (solid line)) behavior and find that only the asymmetric description as shown in Fig. 3 as the solid line describes the data for positive current densities well.

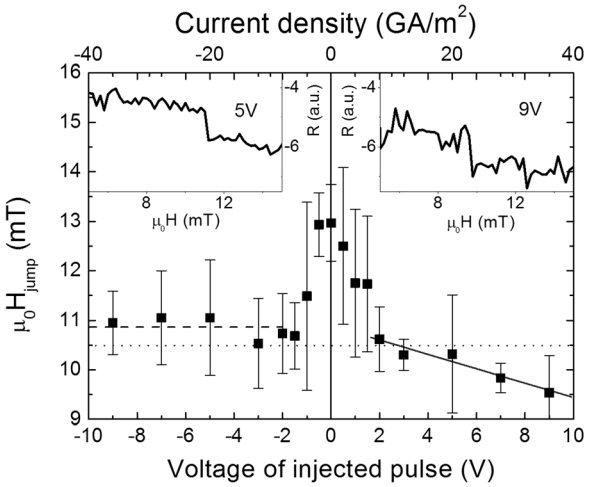

FIG. 3. Depinning fields for the domain wall in the LSMO half ring as determined from the jump in the resistance signal. Data shown is averaged over six measurements in different experimental runs each, with error bars corresponding to one standard deviation. The lines correspond to different fits of high current density data (assuming either symmetric or asymmetric behavior). The insets show examples of two depinning field measurements for 5 V and 9 V pulses, showing also the increase in the resistance fluctuations.

This unipolar reduction of the depinning field is the signature of current assisted magnetic domain wall depinning due to the spin torque effect. A constant depinning field for opposite (negative current density) pulses is expected (and has been observed previously for 3*d* metals[28]) for STT, because the magnetic field is applied permanently while current pulses act only during a short period of time. Hence for field and current acting in opposite directions the wall depins in between current pulses at the same field.

Next we use the difference in the depinning fields for opposite current polarities to estimate the STT efficiency and thus the non-adiabaticity parameter. From the slope of the depinning field *vs.* current density (i.e., the slope of the solid line in Figure 3), we calculate the STT effect in these LSMO structures as $\varepsilon = 4 \times 10^{-14}$ Tm^2/A. This value is 5–10 times larger than typical values for permalloy,[28] showing a larger spin torque efficiency for LSMO.

Assuming a spin polarization P close to 100%,[29] a saturation magnetization of $M_s = 320$ kA/m obtained from SQUID data for an equivalent LSMO thin film[30] and using a domain wall width Δ of 0.5 μm, which we determined from PEEM measurements for 2 μm wide ring structures,[13,14] we obtain from[26]

$$\varepsilon = \frac{\pi \beta P \hbar}{2 e M_s \Delta},$$

a nonadiabaticity $\beta = 5.8$. This value is much higher than the damping constant $\alpha \leq 0.01$ obtained from ferromagnetic resonance measurements (FMR),[31] indicating that spin relaxation is not the only mechanism contributing to the non-adiabaticity, but that a further mechanism plays a decisive role.[9]

Finally, for higher injected current densities, starting at around 20 GA/m^2, we find that each current injection can change the measured resistance level. Both positive and

negative changes in the resistance are observed, which correspond to random modifications of the magnetization, most likely induced by the current injection due to temporary heating close to and above the Curie temperature. The fact that these resistance changes are of magnetic origin is corroborated by the fact that after applying an external field to reinitialize the spin structure, the original resistance level is recovered, excluding permanent modifications of the structure, e.g., by electromigration. Once these fluctuations in the resistance levels become comparable to the change in resistance between the presence and absence of a domain wall, we cannot reliably detect the domain wall depinning anymore. An example of a curve for a medium current density (5 V) and a high current density where fluctuations become large (9 V) are shown as insets in Fig. 3.

In conclusion, we have performed measurements of current assisted magnetic domain wall depinning in LSMO wire structures. We have observed and discriminated heating effects by using different current polarities at low current density as well as a reduction of the depinning field at moderately higher, positive current density, indicating a STT effect. The STT efficiency in our sample is in the order of 4×10^{-14} Tm^2/A which is 5–10 times higher than typical values for permalloy. The deduced non-adiabaticity parameter is more than 10 times higher than in permalloy and much higher than the damping constant showing that spin relaxation is not the dominating mechanism leading to this non-adiabaticity. Finally heating effects play a considerable role, probably due to the higher resistivity of LSMO compared to 3*d* metals together with the lower Curie temperature. So while the spin torque efficiency is high, the low Curie temperature will mean that good cooling mechanisms are needed to use this efficiency and implementation in a room temperature device will be challenging.

This work was funded by EU's 7th Framework Programme IFOX (Nos. NMP3-LA-2010 and 246102), MAGWIRE (No. FP7-ICT-2009-5 257707), the European Research Council through the Starting Independent Researcher Grant MASPIC (No. ERC-2007-StG 208162), the Swiss National Science Foundation, the Graduate School of Excellence "Materials Science in Mainz" (No. GSC266), and the Deutsche Forschungsgemeinschaft (DFG).

[1]J. C. Slonczewski, J. Magn. Magn. Mater. **159**, L1 (1996).
[2]L. Berger, Phys. Rev. B **54**, 9353 (1996).
[3]J. A. Katine, F. J. Albert, R. A. Buhrman, E. B. Myers, and D. C. Ralph, Phys. Rev. Lett. **84**, 3149 (2000).
[4]A. Yamaguchi, T. Ono, S. Nasu, K. Miyake, K. Mibu, and T. Shinjo, Phys. Rev. Lett. **92**, 077205 (2004).
[5]J. Grollier, P. Boulenc, V. Cros, A. Hamzić, A. Vaurès, A. Fert, and G. Faini, Appl. Phys. Lett. **83**, 509 (2003).
[6]M. Kläui, C. A. F. Vaz, J. A. C. Bland, W. Wernsdorfer, G. Faini, E. Cambril, and L. J. Heyderman, Appl. Phys. Lett. **83**, 105 (2003).
[7]H. Numata, T. Suzuki, N. Ohshima, S. Fukami, K. Nagahara, N. Ishiwata, and N. Kasai, Dig. Tech. Pap. Symp. VLSI Technol. **2007**, 232.
[8]S. S. P. Parkin, M. Hayashi, and L. Thomas, Science **320**, 190 (2008).
[9]O. Boulle, G. Malinowski, and M. Kläui, Mater. Sci. Eng., R **72**, 159 (2011).
[10]A. Thiaville, Y. Nakatani, J. Miltat, and Y. Suzuki, Europhys. Lett. **69**, 990 (2005).
[11]A. Biehler, M. Kläui, M. Fonin, C. König, G. Güntherodt, and U. Rüdiger, Phys. Rev. B **75**, 184427 (2007).
[12]M. Fonin, C. Hartung, U. Rüdiger, D. Backes, L. Heyderman, F. Nolting, A. F. Rodríguez, and M. Kläui, J. Appl. Phys. **109**, 07D315 (2011).
[13]J. Rhensius, C. A. F. Vaz, A. Bisig, S. Schweitzer, J. Heidler, H. S. Körner, A. Locatelli, M. A. Niño, M. Weigand, L. Méchin, F. Gaucher, E. Goering, L. J. Heyderman, and M. Kläui, Appl. Phys. Lett. **99**, 062508 (2011).
[14]J. Heidler, J. Rhensius, C. A. F. Vaz, P. Wohlhüter, H. S. Körner, A. Bisig, S. Schweitzer, A. Farhan, L. Mechin, L. Le Guyader, F. Nolting, A. Locatelli, T. O. Mentes, M. A. Nino, F. Kronast, L. J. Heyderman, and M. Kläui, J. Appl. Phys. **112**, 103921 (2012).
[15]H. Boschker, M. Huijben, A. Vailionis, J. Verbeeck, S. van Aert, M. Luysberg, S. Bals, G. van Tendeloo, E. P. Houwman, G. Koster, D. H. A. Blank, and G. Rijnders, J. Phys. D: Appl. Phys. **44**, 205001 (2011).
[16]T. Arnal, A. V. Khvalkovskii, M. Bibes, B. Mercey, Ph. Lecoeur, and A.-M. Haghiri-Gosnet, Phys. Rev. B **75**, 220409(R) (2007).
[17]L. Pallechi, L. Pellegrino, A. Caviglia, E. Bellingeri, G. Canu, G. C. Gazzadi, A. S. Siri, and D. Marre, Phys. Rev. B **74**, 014434 (2006).
[18]A. Rutolo, A. Oropallo, F. M. Granozio, G. P. Pepe, P. Perna, and U. Scotti di Uccio, Appl. Phys. Lett. **91**, 132502 (2007).
[19]L. Mechin, S. Wu, B. Guillet, P. Perna, C. Fur, S. Lebargy, C. Adamo, D. G. Schlom, and J. M. Routoure, J. Phys. D: Appl. Phys. **46**, 202001 (2013).
[20]V. Moshnyaga, I. Khoroshun, A. Sidorenko, P. Petrenko, A. Weidinger, M. Zeitler, B. Rauschenbach, R. Tidecks, and K. Samwer, Appl. Phys. Lett. **74**, 2842 (1999).
[21]M. Kläui, C. A. F. Vaz, J. Rothman, J. A. C. Bland, W. Wernsdorfer, G. Faini, and E. Cambril, Phys. Rev. Lett. **90**, 097202 (2003).
[22]See supplementary material at http://dx.doi.org/10.1063/1.4865415 for the measured AMR curve of the investigated LSMO sample and a magnetic microscopy image of a similar LSMO halfring structure. The Photo emission electron micoscopy (PEEM) imaging was performed on the SIM-X11MA beamline at the Swiss Light Source, Paul Scherrer Institut, Villigen, Switzerland.
[23]X. W. Li, A. Gupta, G. Xiao, and G. Q. Gong, Appl. Phys. Lett. **71**, 1124 (1997).
[24]C. A. F. Vaz, E. Blackburn, M. Kläui, J. A. C. Bland, L. Gan, W. F. Egelhoff, E. Cambril, G. Faini, and W. Wernsdorfer, J. Appl. Phys. **93**, 8104 (2003).
[25]M. Kläui and C. A. F. Vaz, in *Handbook of Magnetism and Advanced Magnetic Materials*, edited by H. Kronmüller and S. S. P. Parkin (Wiley, New York, 2007), Vol. 2, p. 879.
[26]O. Boulle, J. Kimling, P. Warnicke, M. Kläui, U. Rüdiger, G. Malinowski, H. J. M. Swagten, B. Koopmans, C. Ulysse, and G. Faini, Phys. Rev. Lett. **101**, 216601 (2008).
[27]J. Heinen, O. Boulle, K. Rousseau, G. Malinowski, M. Kläui, H. J. M. Swagten, B. Koopmans, C. Ulysse, and G. Faini, Appl. Phys. Lett. **96**, 202510 (2010).
[28]M. Laufenberg, W. Bührer, D. Bedau, P.-E. Melchy, M. Kläui, L. Vila, G. Faini, C. A. F. Vaz, J. A. C. Bland, and U. Rüdiger, Phys. Rev. Lett. **97**, 046602 (2006).
[29]J.-H. Park, E. Vescovo, H.-J. Kim, C. Kwon, R. Ramesh, and T. Venkatesan, Nature **392**, 794 (1998).
[30]R. M. Reeve, C. Mix, M. König, M. Foerster, G. Jakob, and M. Kläui, Appl. Phys. Lett. **102**, 122407 (2013).
[31]A. Monsen, Ph.D. thesis, Norwegian University of Science and Technology, 2012; E. Wahlström, private communication (2013).